Talanta 107 (2013) 408–415

Contents lists available at SciVerse ScienceDirect

Talanta

journal homepage: www.elsevier.com/locate/talanta

Size-dependent cellular uptake efficiency, mechanism, and cytotoxicity of silica nanoparticles toward HeLa cells

Jie Zhu [a,1], Lei Liao [a,1], Lina Zhu [a], Peng Zhang [a], Kai Guo [a], Jilie Kong [a], Chang Ji [b], Baohong Liu [a,*]

[a] Department of Chemistry and Institute of Biomedical Sciences, Fudan University, Shanghai 200433, China
[b] Department of Chemistry and Biochemistry, Texas State University—San Marcos, San Marcos, TX 78666, USA

ARTICLE INFO

Article history:
Received 13 November 2012
Received in revised form
22 January 2013
Accepted 23 January 2013
Available online 29 January 2013

Keywords:
Silica nanoparticles
Cell uptake
Particle size
Cytotoxicity

ABSTRACT

In this study, we investigated and reported the cellular uptake efficiency, mechanism, and cytotoxicity of silica nanoparticles (SNPs) with different sizes. Using confocal laser scanning microscope (CLSM), flow cytometry (FCM), and graphite furnace atomic absorption spectrometry (GFAAS), the qualitative and quantitative experimental results showed that the cellular uptake of SNPs toward HeLa cells is size-dependent. To further examine the uptake process, three different inhibitors including sucrose, Filipin III, and Cytochalasin D (Cyt D) were introduced to pretreat the HeLa cells. It appeared that the largest SNPs (SNPs-307.6) take an energy-dependent uptake pathway (clathrin dependent and caveolin independent) while that for the medium size SNPs-167.8 involves clathrin and caveolin dependent endocytosis. In contrast, the smallest SNPs (SNPs-55.6) follow not only energy required clathrin and caveolin dependent endocytosis but also an energy independent pathway to efficiently enter the cells. Moreover, the cellular uptake efficiency of SNPs, which also show excellent biocompatibility, is size-dependent in the order of 55.6 > 167.8 > 307.6 nm. This knowledge is fundamentally important and will facilitate more development of size-defined SNPs as the transporters for various purposes.

1. Introduction

Silica nanomaterials have been investigated for their biomedical applications in drug release [1,2], biosensing [3,4], and as interesting candidates for injectable nanovectors [5–7]. Solid siliceous nanoparticles, typically synthesized by Stober's method [8], can be functionalized and developed for DNA delivery [9]. Mesoporous silica nanoparticles (MSNs) with tunable particle size, morphology, and porosity as well as different surface functional groups have become highly attractive in a wide range of promising technologies, such as catalysis [10], separation [11], controlled release [12–14], and bioapplications [15–18]. In particular, these nanomaterials have been developed as carriers to deliver drugs and DNAs into the cells of human beings, animals, and plants with excellent biocompatibility [15,19].

Although many applications have shown promising potential in disease diagnosis and therapy, the fundamental interactions of SNPs with cells still remain unknown, for a large part. It was reported that the internalization of fluorescein isothiocyanate (FITC) modified SNPs, which is mediated by clathrin and actin dependent endocytosis in both human mesenchymal stem cells (hMSCs) and 3T3-L1 cells, is concentration-, time-, and cell type-dependent [20]. The possible mechanisms were studied for the cellular uptake of this material in the presence of specific endocytic trafficking inhibitors. It was demonstrated that the uptake of FITC-modified silica nanoparticles is energy-dependent through a clathrin mediated pathway toward HeLa cells and human pancreatic cancer cell line (PANC-1) [21,22].

Further studies revealed that the surface charge on SNPs can not only influence ED50 (the value for the effective dose at 50% of internalization) but also the mechanisms of internalization [20,21]. After surface modification, the silica nanoparticles may be internalized through a caveolin mediated process [21]. The effect of surface charge on the cellular uptake of SNPs toward hMSCs and 3T3-L1 cells was reported by Huang et al. [20]. Their results showed that the uptake of SNPs by hMSCs can be regulated by a threshold of positive surface charge and the modulation of surface charge on the uptake is specific to cell type.

Besides the surface charge, the size of SNPs is another important factor which can affect the cellular uptake. It was reported that SNPs with a diameter of 50 nm could be the most suitable candidate to serve as a carrier into the cells [23]. Our previous work demonstrated that the ultra small hollow SNPs possess enhanced endocytosis properties when compared to conventional ones with relatively larger particle sizes [24]. It has also been shown that SNPs with a diameter of 50 nm or less can enter the nucleus and may be used in the application for

* Corresponding author. Tel.: +86 21 65642009; fax: +86 21 65641740.
E-mail address: bhliu@fudan.edu.cn (B. Liu).
[1] Jie Zhu and Lei Liao contributed equally to this work.

0039-9140/$ - see front matter © 2013 Elsevier B.V. All rights reserved.
http://dx.doi.org/10.1016/j.talanta.2013.01.037

improving the efficiency of anticancer drug delivery [25]. However, as far as it is concerned, the size effect of SNPs on the cellular uptake mechanism has not been studied in detail.

To facilitate theoretical and experimental investigations, studies for cellular uptake of SNPs with consistency in Zeta potential and surface functionality are desired to elucidate the effect of size on the efficiency, mechanism, and cytotoxicity of the uptake process. Herein, we focused on examining the cellular uptake pathway as well as the corresponding efficiency and cytotoxicity of SNPs with similar surface charges but different sizes, in order to get insight into the intracellular properties of SNPs. Interestingly, we discovered that SNPs with different diameters do follow different uptake pathways and the subcellular localization of internalized materials is also size-dependent. We propose that silica nanoparticles with a diameter of less than 160 nm (which can enter the cell but not likely the nucleus) might be candidates for drug delivery and those SNPs having a diameter of 50 nm or less (which can enter the nucleus) could be carriers of siRNA and DNA for gene therapy. Nevertheless, there is no "rule of thumb" to predict which endocytic pathway that either SNPs or functionalized SNPs will follow when internalized by the cells. To further understand the pathway for cellular internalization of SNPs will be of utmost importance for many of its applications in biotechnology and biomedicine.

2. Materials and methods

2.1. Materials

All chemicals were used as received without further purification. Filipin III and Cytochalasin D (Cyt D) were purchased from Sigma-Aldrich. The HeLa cell line was provided by the Institute of Biochemistry and Cell Biology, SIBS, CAS (China). Cetyltrimethylammonium chloride (CTAC), tetraethoxysilane (TEOS), 3-aminopropyltrimethoxysilane (APTMS), diethanolamine (DEA), ammonium hydroxide (NH_4OH), ethanol, and sucrose were purchased from Shanghai Chemical Corp.

2.2. Synthesis of SNPs

The mesoporous silica nanoparticles used in this work were synthesized according to literature procedures [26]. For the synthesis of SNPs-55.6, 7.2 mL of water, 0.9 g of ethanol, 0.26 g of CTAC, and 0.02 g of DEA were mixed and stirred in a water bath at 40 °C for 30 min. Subsequently, 0.73 mL of TEOS was added dropwise within 2 min under stirring. For the synthesis of SNPs-167.8, the same procedure was followed except that the amount of ethanol used was 1.65 g. The solution gradually turned to white and was stirred for another 2 h. The milky mixture was allowed to undergo dialysis for 48 h. The white powders were collected after evaporation of the solvent. The final products were obtained after calcination at 550 °C for 5 h. For the synthesis of SNPs-307.6 [8], 5.1 g of NH_4OH solution and 4.5 g of water were added to 38 g of ethanol. Afterwards, 2.08 g of TEOS was added dropwise within 2 min under stirring. With further stirring for 12 h, the milky mixture was centrifuged and the product was obtained by evaporation of the solvent.

2.3. Synthesis of FITC–SNPs

5 mg of FITC was mixed with 10 μL of APTMS and stirred for 2 h. The mixture was added to the aqueous solution of SNPs and allowed to react for another 2 h. The unreacted FITC and APTMS were removed by dialysis for 48 h.

2.4. Characterization

Transmission electron microscopy (TEM) images were obtained with the aid of a JEOL 2011 microscope operated at 200 kV. Scanning electron microscopy (SEM) images were collected by a Philips XL30 microscope operated at 20 kV. The size distribution and Zeta potential of SNPs were measured by dynamic light scattering (DLS) at 25 °C using Nanosizer ZS-90 (Malvern). Nitrogen sorption isotherms were measured at 77 K by a Micromeritics Tristar 3000 analyzer. Small-angle X-ray scattering (SAXS) patterns were recorded by a Bruker D4 X-ray diffractometer with Ni-filtered

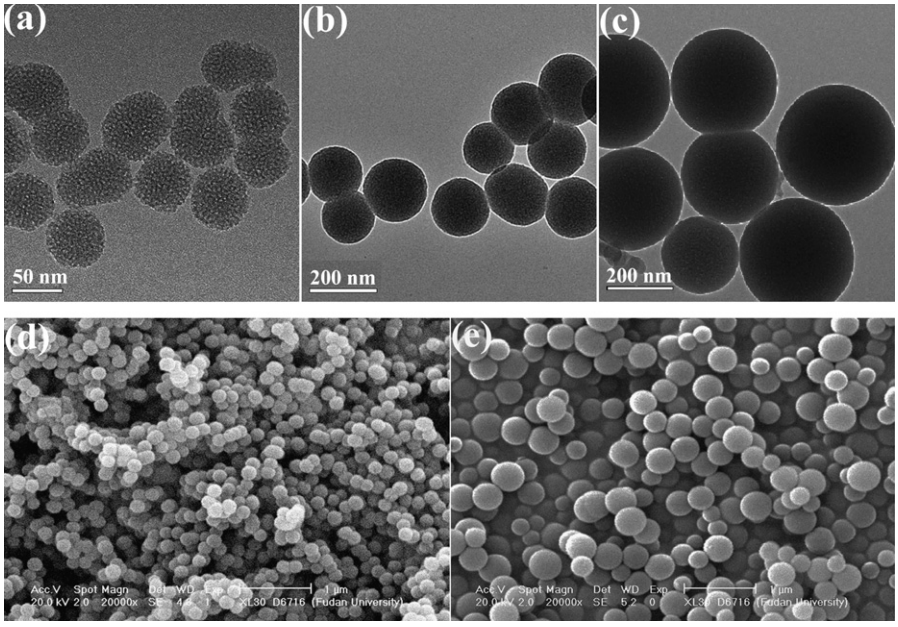

Fig. 1. TEM images of FITC functionalized: (a) SNPs-55.6; (b) SNPs-167.8; and (c) SNPs-307.6. SEM images of FITC functionalized: (d) SNPs-167.8 and (e) SNPs-307.6.

Cu Kα radiation ($\lambda = 1.54056$ Å) at a voltage of 40 kV and a current of 40 mA.

2.5. Cellular uptake

HeLa cells were incubated with 40 μg/mL SNPs in a serum free medium for 3 h at 4 °C or 37 °C under 5% CO_2. After incubation, the cells were fixed with 4% paraformaldehyde and the nuclei were stained with 5 μg/mL 4′,6-diamidino-2-phenylindole (DAPI) in 10% glycerol. Confocal fluorescence images were obtained by a confocal laser scanning microscope (CLSM) imaging system (Leica TCS SP5) and a 63× oil-immersion objective lens. Excitation at 488 nm was provided by a Multi Ar laser. For flow cytometry (FCM), the cells were harvested by trypsinization and the analysis was carried out by an EPICS ALTRA automatic flow cytometer (Beckman Coulter). HeLa cells were also placed in Modified Eagle′s Medium (MEM) on 14-mm glass coverslips (5×10^8 cells/L for CLSM) or in 60-mm tissue culture dishes (5×10^5 cells/dish for FCM) supplemented with 10% Fetal Bovine Serum (FBS) at 37 °C under 5% CO_2 and allowed to grow for 24 h. After incubation, the cells were washed with phosphate buffer solutions (PBS, pH = 7.4) for three times. Serum free media containing 0.45 mol/L sucrose, 5 mg/L filipin III, or 1 μmol/L Cyt D were then added, respectively. The HeLa cells were incubated afterwards with 40 μg/mL SNPs for 3 h at 37 °C under 5% CO_2 before CLSM and FCM analyses. For graphite furnace atomic absorption spectrometry (GFAAS) analyses, HeLa cells were seeded in a 10-cm Petri dish (2×10^6 cells/dish) and cultivated with 40 μg/mL SNPs for 3 h. Subsequently, the cells were washed with PBS for three times and trypsinized. After centrifugation and being washed once, the cells were resuspended in water and centrifuged again for collection. They were dried overnight before 100 μL of 48–51 wt% HF and 9.9 mL of 2 wt% HNO_3 were added sequentially to allow dissolution of the SNPs and cells with the aid of sonication. The mass of FITC–SNPs in the HeLa cells was determined by measuring the silicon concentration using GFAAS (Unicam Solar 939).

2.6. Cytotoxicity

Cell viability was determined by MTT assay. Cells were placed in a 96-well flat bottom plate with 6×10^3 cells per well and allowed to grow overnight prior to exposure to SNPs at different concentrations. After 48 h of incubation, the MTT reagent was added to be converted to a purple formazan product by active mitochondria for 4 h at 37 °C. The product was then dissolved in DMSO and quantified by absorption spectrophotometry at 490 nm with the aid of an enzyme-labelled instrument (SUNOS-TIK SPR-960).

Table 1
Zeta potentials of the SNPs before and after the surface modification with FITC.

Materials	Zeta potentials (mV)
SNPs (55.6 nm)	−25.4
FITC–SNPs (55.6 nm)	−23.8
SNPs (167.8 nm)	−24.0
FITC–SNPs (167.8 nm)	−23.0
SNPs (307.6 nm)	−27.3
FITC–SNPs (307.6 nm)	−27.0

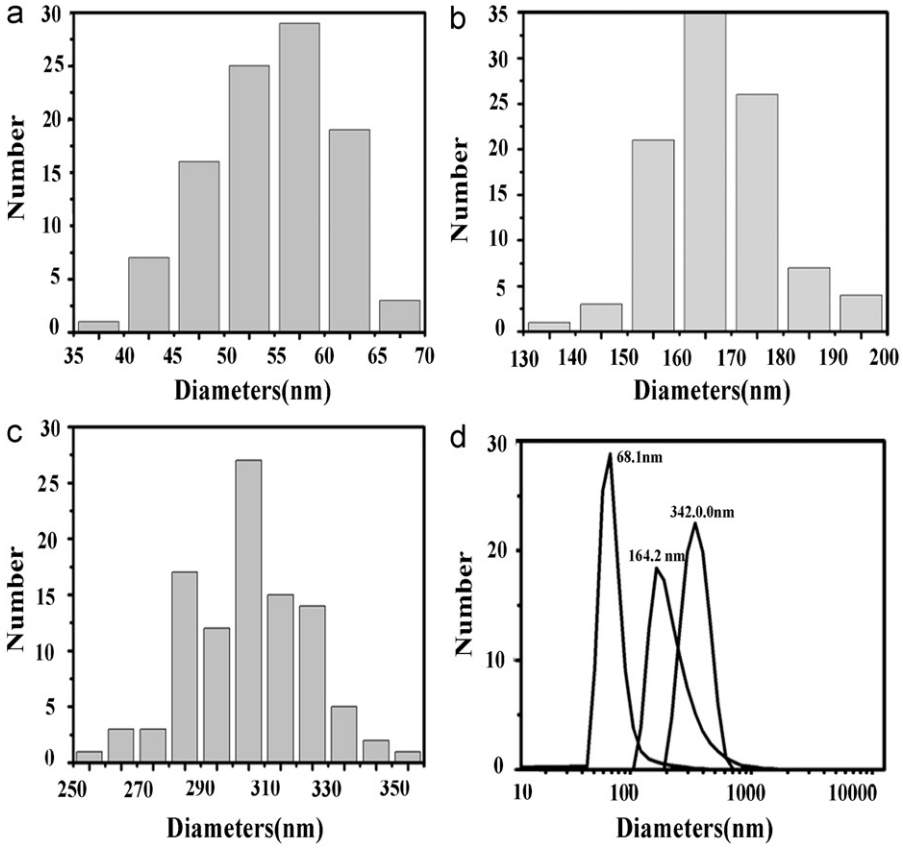

Fig. 2. The histograms showing the size distributions of 100: (a) SNPs-55.6; (b) SNPs-167.8; and (c) SNPs-307.6 measured by TEM as well as (d) the size distributions of SNPs measured by Nanosizer ZS-90.

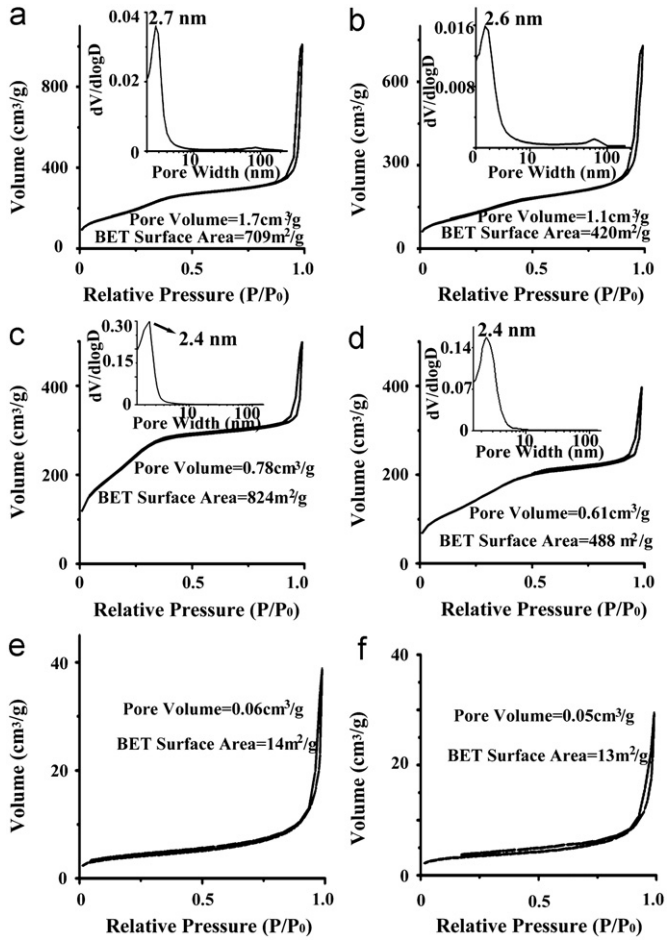

Fig. 3. Nitrogen adsorption–desorption isotherms of: (a) SNPs-55.6; (b) FITC–SNPs-55.6; (c) SNPs-167.8; (d) FITC–SNPs-167.8; (e) SNPs-307.6; and (f) FITC–SNPs-307.6.

3. Results and discussion

3.1. Characterization of SNPs

SNPs with different sizes were synthesized according to the literatures [8,26]. In order to compare the cellular uptake performance of various SNPs and study the corresponding intracellular uptake mechanisms, FITC was covalently linked to the surface of SNPs for fluorescence detection. TEM and SEM images of FITC functionalized SNPs (FITC–SNPs) are shown in Fig. 1. By measuring the diameters of 100 individual SNPs directly from the TEM images, the narrow size distributions of approximately 55.6 nm (SNPs-55.6), 167.8 nm (SNPs-167.8), and 307.6 nm (SNPs-307.6) are presented in Fig. 2a–c. Comparatively, DLS analyses showed that the diameters of the three SNPs in phosphate buffer solutions (PBS, pH=7.4) are centered at 61.8 nm, 164.2 nm, and 342.0 nm (Fig. 2d), which are slightly larger than the results obtained from TEM images except that of SNPs-167.8. This is reasonable because hydrodynamic diameters are generally larger than the core nanoparticle sizes observed by TEM [23].

Since previous data revealed that the surface charge can not only affect the ability of SNPs to internalize cells and escape endosomal entrapment [21] but also the corresponding cellular uptake mechanisms [20,21], the surface charges on the three SNPs were measured to check the uniformity of this parameter. Table 1 shows the Zeta potentials for various SNPs suspended in PBS before and after the surface modification with FITC. When compared with those of SNPs-55.6 and SNPs-167.8, the Zeta potential of SNPs-307.6 is a little more negative. This small difference can be attributed to the condensation of silanol groups of hydrated SNPs-55.6 and SNPs-167.8 during the calcination process [24]. After modification with FITC, the surface charges on FITC–SNPs increase slightly due to the presence of amino groups (from APTMS used to treat SNPs surface) which are not linked to FITC. In general, the surface charges are similar for FITC–SNPs of different sizes at the physiological pH. Fig. 3 shows the nitrogen adsorption–desorption isotherms of the SNPs before and after the

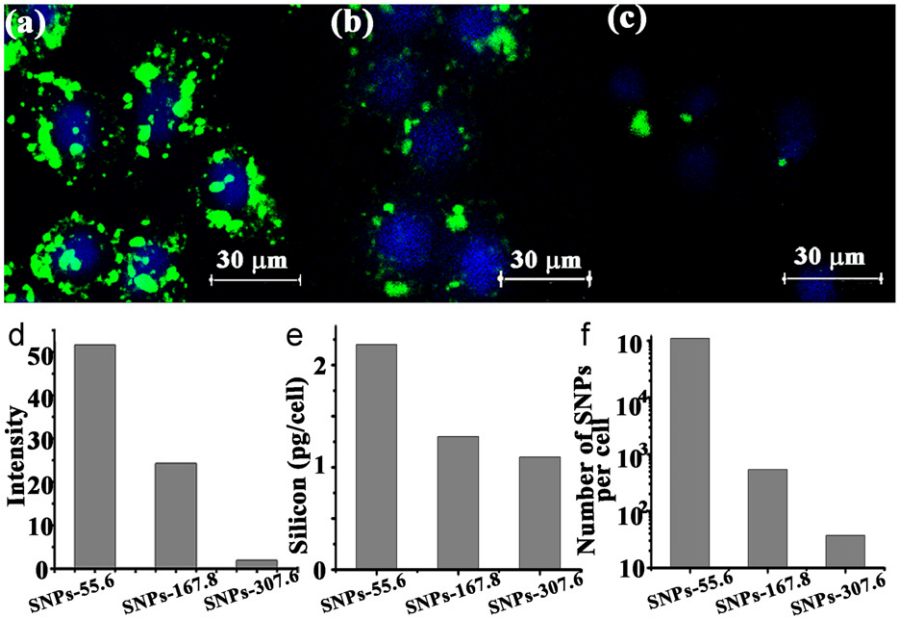

Fig. 4. Fluorescence confocal micrographs of HeLa cells cultivated with: (a) SNPs-55.6; (b) SNPs-167.8; and (c) SNPs-307.6 for 3 h at 37 °C. (d) The FCM results for HeLa cells cultivated with SNPs-55.6, SNPs-167.8, and SNPs-307.6 for 3 h at 37 °C. Uptake efficiency for various SNPs toward HeLa cells was measured three times by GFAAS to give the average (e) concentration of silicon per cell and (f) number of SNPs internalized per cell.

surface modification with FITC. The total pore volumes decrease slightly due to the surface functionalization. The SAXS patterns are also presented in the supporting information (Fig. S1).

3.2. Size effect of SNPs on cellular uptake

We first investigated the size effect on cell labeling (shown in Fig. 4). The uptake of various sizes of FITC–SNPs by HeLa cells was examined by CLSM, FCM, and GFAAS. It has been reported that the uptake of SNPs begins within 30 min of incubation and is relatively rapid for the first 1–2 h [20]. Since uptake saturation could be usually achieved after 2 h of incubation [20], we chose 3 h of incubation time for the HeLa cells cultivated with FITC–SNPs in different sizes at 37 °C. The CLSM studies revealed that the intensity of green fluorescence for SNPs-55.6 is much stronger than those for SNPs-167.8 and SNPs-307.6, and that for SNPs-307.6 is the weakest. More interestingly, SNPs-55.6 were found to transport through the nuclear envelope (Fig. 4a), which is consistent with our previous reports [27]. The confocal microscopy Z-scan image series of one HeLa cell (Fig. 5) clearly revealed that SNPs-55.6 has not only been transported into the cytoplasma of cells, but also the nucleus (Fig. 5). More recently, it was reported that SNPs with a diameter of 50 nm or less can efficiently target the nucleus to deliver the active anticancer drug and kill the cancer cell much more effectively [25]. The FCM results also indicated that the cellular uptake is highly size-dependent in the order of 55.6 > 167.8 > 307.6 nm (Fig. 4d).

FCM and GFAAS are the two conventional techniques used to quantitatively compare the uptake efficiency for various SNPs. However, the three SNPs employed in this study have huge differences in specific surface areas, which will inevitably affect the amounts of chemically linked FITC (attached to silanol groups on surface) per unit weight of silica. Consequently, FCM can only provide the quantitative information of the FITC concentration in the cell, which is not a direct measurement for the uptake efficiency of SNPs. To solve this problem, GFAAS was used to directly quantitate the amounts of SNPs internalized in HeLa cells [24]. Fig. 4e shows that the mass of silicon internalized per cell obtained from GFAAS measurements is 2.2, 1.3, and 1.1 pg/cell for SNPs-55.6, SNPs-167.8, and SNPs-307.6, respectively. The number of SNPs internalized by each cell (n) may also be estimated. For approximation, the nanoparticles are taken as spheres and n can be simply calculated by $n=[(m/p)+mV]/(4/3)\pi r^3$, where m represents the mass of silica per cell which is determined by Fig. 3e, ρ is the density of amorphous silica ($\sim$2.2 g/cm^3), V is the pore volume measured by nitrogen sorption analysis, and r is the radius of nanoparticles [24]. As given in Fig. 4f, the number of SNPs-55.6 internalized per cell (1.1×10^5) is two–three-orders of magnitude more than that of SNPs-167.8 (5.4×10^2) or SNPs-307.6 (3.7×10^1). These results confirmed that the uptake efficiency of SNPs is indeed size-dependent in the order of 55.6 > 167.8 > 307.6 nm.

3.3. Study of uptake mechanism for SNPs with various sizes

Eukaryotic cells internalize extracellular materials inside cytoplasm through energy independent or energy-dependent uptake pathway [28–30]. Generally, low molecular weight solutes directly

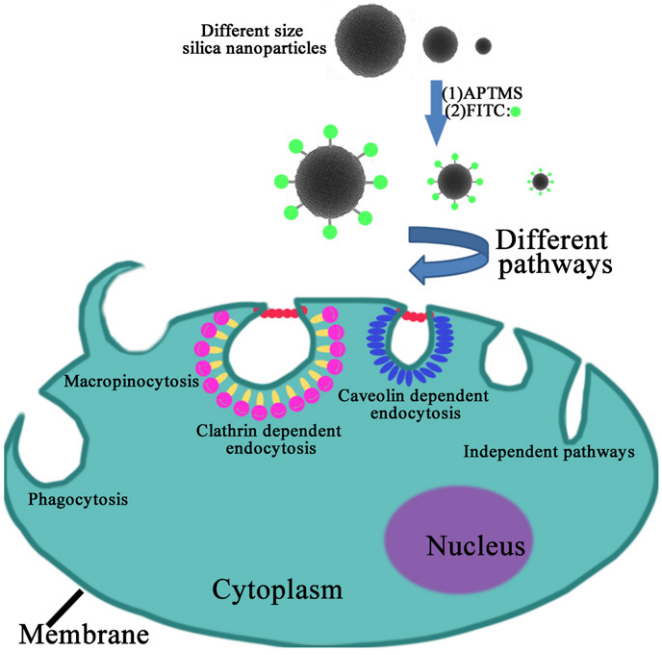

Scheme 1. Large particles are internalized by phagocytosis, whereas fluid uptake occurs by macropinocytosis. In the case of silica nanoparticles, most internalization is via endocytic pathways which could be different with regard to the nature of the surface functionalization and structural properties of SNPs [32].

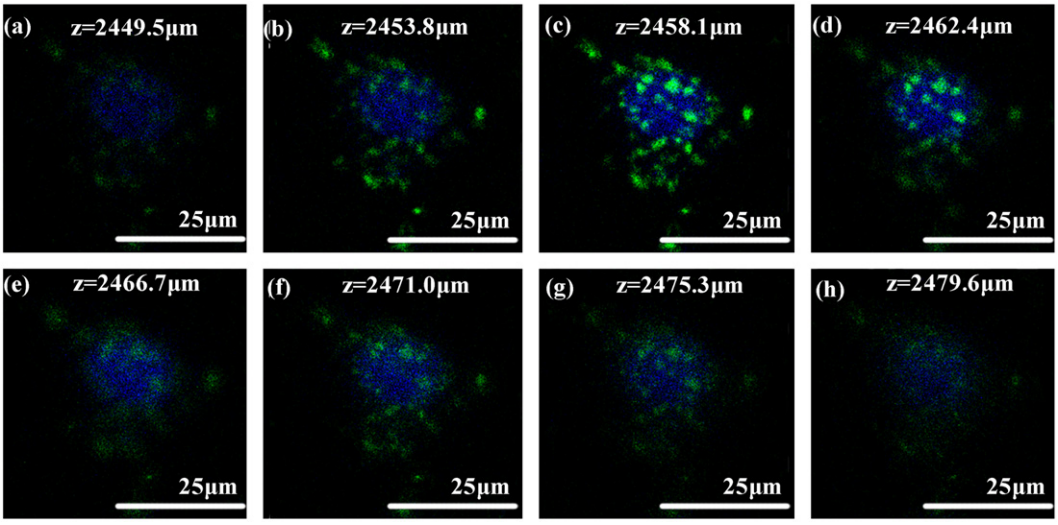

Fig. 5. The confocal microscopy Z-scan image series of one HeLa cell cultivated with SNPs-55.6. The blue region represents the nucleus. (For interpretation of the references to color in this figure legend, the reader is referred to the web version of this article.)

transport through the plasma membrane without consuming energy via the energy independent pathway. The energy-dependent pathway, also known as endocytosis for uptake of relatively large particles, can be hindered when incubations are performed at 4 °C. The endocytosis is divided into at least three subcategories: clathrin dependent, caveolin dependent, and clathrin/caveolin independent [31,32]. Extracellular materials or solutes following the clathrin dependent uptake pathway are first enclosed within clathrin coated vesicles derived from folds or invaginations of the plasma membrane, and then brought into the cells. Sucrose can disturb the formation of clathrin coated vesicles on the cell membrane and thus hinder the clathrin dependent endocytosis [33–35]. On the other hand, clathrin independent endocytosis can occur through the caveolae or lipid rafts. Filipin interacts with 3-β-hydroxysterols in the plasma membrane to form filipin–sterol complexes which subsequently cause the filamentous caveolin-1-coat to rapidly disassemble, leading to inhibition of caveolin mediated endocytosis [35,36]. Cyt D, a potent inhibitor of actin polymerization, was used to inhibit actin related phagocytosis and clathrin/caveolin independent endocytosis [32,37]. In the case of SNPs, most internalization is via endocytic pathways which could be different with regard to the nature of the surface functionalization and structural properties of SNPs (shown in Scheme 1) [38,39]. Once the silica nanoparticles have overcome the cell membrane barrier, they have to reach the cytoplasm to release the cargoes. To understand the corresponding intracellular pathways would help the design of more efficient drug delivery systems.

Fig. 6 presents the CLSM and FCM data for HeLa cells after 3 h of incubation in solutions containing SNPs with various sizes under different conditions. Cells incubated at 37 °C without adding any SNPs were used as a control group. By incubating cells with SNPs at different temperatures, we found that the uptake of silica nanoparticles is higher at 37 °C than at 4 °C. The CLSM for HeLa cells cultivated with SNPs-307.6 at 4 °C does not give any green fluorescence and the relative fluorescence intensity obtained from FCM is 0.6, which is very close to the control group (0.4) and indicates that the uptake of SNPs-307.6 is through

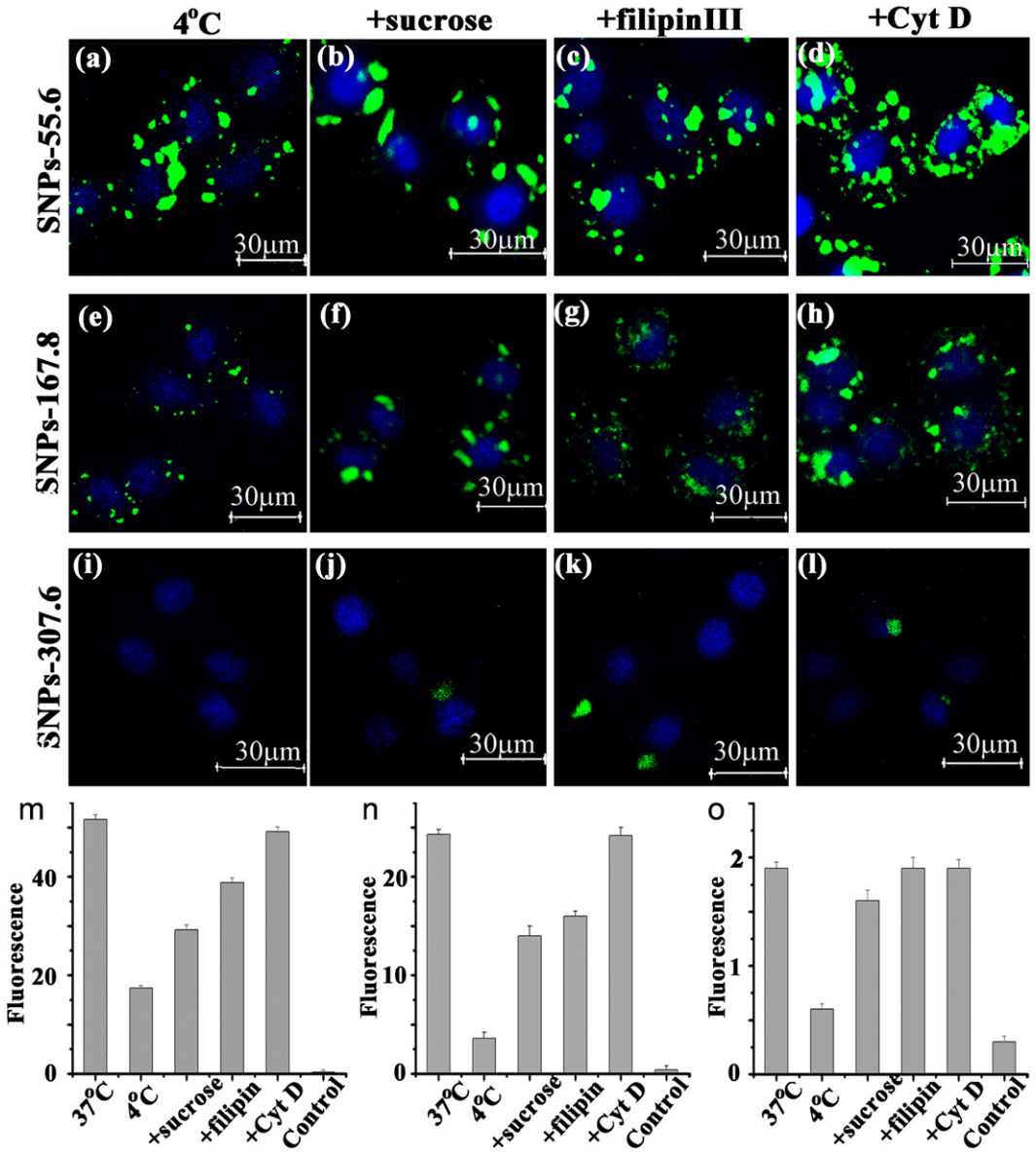

Fig. 6. Fluorescence confocal micrographs of HeLa cells cultivated with: (a–l) SNPs-55.6, SNPs-167.8, and SNPs-307.6 for 3 h at 4 °C or at 37 °C with different pretreatments and the FCM results for HeLa cells cultivated with (m) SNPs-55.6, (n) SNPs-167.8, and (o) SNPs-307.6 for 3 h at 4 °C or at 37 °C with different pretreatments. CLSM and FCM measurements were repeated for three times.

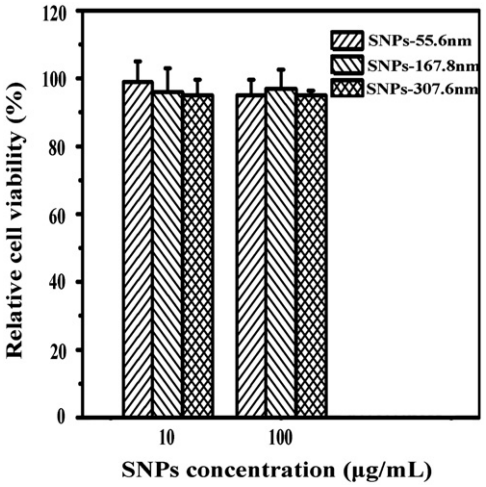

Fig. 7. Relative cell viability (versus untreated control) data for HeLa cells incubated with SNPs-55.6, SNPs-167.8, and SNPs-307.6 at different concentrations for 48 h.

an energy-dependent pathway [25,27,40]. Green fluorescence can be observed for the two smaller SNPs from both CLSM and FCM but the intensity for HeLa cells cultivated with SNPs-55.6 at 4 °C is more obvious. The relative fluorescence intensities in FCM for HeLa cells cultivated with SNPs-55.6 and SNPs-167.8 at 37 °C were measured to be 51.6 and 24.3, while those for HeLa cells cultivated at 4 °C decreased to 17.4 and 3.6, respectively. Nevertheless, those results at incubation temperature of 4 °C are still higher than the control, suggesting that the two smaller SNPs should also follow an energy independent pathway besides the energy-dependent pathway, especially for SNPs-55.6 [40].

Three different inhibitors including sucrose, Filipin III, and Cyt D were used for cell pretreatments to study the endocytosis mechanisms for various SNPs. The resulting effects on fluorescence intensity were examined and compared with those cultivated at 37 °C without any pretreatment. As shown in Fig. 6, the relative fluorescence intensities in FCM for cells with the pretreatment of sucrose decrease from 51.6 to 29.2 for SNPs-55.6, 24.3 to 14.0 for SNPs-167.8, and 1.9 to 1.6 for SNPs-307.6. These results indicate that the cellular uptake of all three SNPs is clathrin dependent [40]. However, with the pretreatment of Filipin III, the relative fluorescence intensity decreases only for SNPs-55.6 and SNPs-167.8, indicating that these two SNPs also follow a caveolin dependent endocytosis pathway. Furthermore, Cyt D does not exert any obvious effect on the cellular uptake of SNPs toward HeLa cells.

In summary, the cellular uptake of SNPs toward HeLa cells is size-dependent. The uptake of the largest SNPs (SNPs-307.6) is through an energy-dependent pathway (clathrin dependent and caveolin independent). While for SNPs-167.8, the process is mainly through energy required clathrin and caveolin dependent endocytosis. On the other hand, the uptake of the smallest SNPs (SNPs-55.6) follows not only clathrin and caveolin dependent endocytosis, but also an energy independent pathway.

3.4. Cytotoxicity of SNPs

To evaluate the *in vitro* cytotoxicity, cell viability was examined by standard MTT assay for various SNPs at two different concentrations (10 μg/mL and 100 μg/mL). As presented in Fig. 7, all SNPs show very low cytotoxicity toward HeLa cells at these concentration levels. The results indicate that the biocompatibility of SNPs is very good.

4. Conclusions

The cellular uptake efficiency, mechanism, and cytotoxicity of SNPs with various sizes toward HeLa cells have been investigated. The endocytosis pathway for large SNPs (307.6 nm) is mainly through clathrin coated pits, while smaller SNPs (167.8 nm) can be internalized through clathrin coated vesicles as well as the caveolin dependent pathway. Furthermore, ultra small SNPs (55.6 nm) can partly enter the cells through an energy independent pathway. The cellular uptake efficiency is also size-dependent in the order of 55.6 > 167.8 > 307.6 nm. On the basis of these results, we propose that silica nanoparticles with a diameter of less than 160 nm (which can enter the cell but not likely the nucleus) might be candidates for drug delivery and those SNPs having a diameter of 50 nm or less (which can enter the nucleus) could be carriers of siRNA and DNA for gene therapy. Further studies may facilitate more development of size-defined SNPs as transporters for different purposes.

Acknowledgments

This research was supported by the NSFC (20925517, 21175028), SKLEAC201101, and Texas State University Faculty Development Leave Program.

Appendix A. Supporting information

Supplementary data associated with this article can be found in the online version at http://dx.doi.org/10.1016/j.talanta.2013.01.037.

References

[1] F. Caruso, Adv. Mater. 13 (2001) 11.
[2] B.G. Trewyn, S. Giri, I.I. Slowing, V.S.Y. Lin, Chem. Commun. 31 (2007) 3236–3245.
[3] Q.S. Huo, J. Liu, L.Q. Wang, Y.B. Jiang, T.N. Lambert, E. Fang, J. Am. Chem. Soc. 128 (2006) 6447–6453.
[4] I.I. Slowing, B.G. Trewyn, S. Giri, V.S.Y. Lin, Adv. Funct. Mater. 17 (2007) 1225–1236.
[5] X.X. He, K.M. Wang, W.H. Tan, B. Liu, X. Lin, C.M. He, D. Li, S.S. Huang, J. Li, J. Am. Chem. Soc. 125 (2003) 7168–7169.
[6] A.H. Nashat, M. Moronne, M. Ferrari, Biotechnol. Bioeng. 60 (1998) 137–146.
[7] F. Yan, R. Kopelman, Photochem. Photobiol. 78 (2003) 587–591.
[8] W. Stöber, A. Fink, J. Colloid Interface Sci. 26 (1968) 62–69.
[9] J.E. Fuller, G.T. Zugates, L.S. Ferreira, H.S. Ow, N.N. Nguyen, U.B. Wiesner, R.S. Langer, Biomaterials 29 (2008) 1526–1532.
[10] J.Y. Ying, C.P. Mehnert, M.S. Wong, Angew. Chem. Int. Ed. 38 (1999) 56–77.
[11] A. Stein, Adv. Mater. 15 (2003) 763–775.
[12] Y.J. Han, G.D. Stucky, A. Butler, J. Am. Chem. Soc. 121 (1999) 9897–9898.
[13] M. Vallet-Regi, F. Balas, D. Arcos, Angew. Chem. Int. Ed. 46 (2007) 7548–7558.
[14] X.M. Jiang, C.J. Brinker, J. Am. Chem. Soc. 128 (2006) 4512–4513.
[15] F. Torney, B.G. Trewyn, V.S.Y. Lin, K. Wang, Nat. Nanotechnol. 2 (2007) 295–300.
[16] B.G. Trewyn, I.I. Slowing, S. Giri, H.T. Chen, V.S.Y. Lin, Acc. Chem. Res. 40 (2007) 846–853.
[17] B. Julian-Lopez, C. Boissiere, C. Chaneac, D. Grosso, S. Vasseur, S. Miraux, E. Duguet, C. Sanchez, J. Mater. Chem. 17 (2007) 1563–1569.
[18] Y.J. Wang, F. Caruso, Chem. Mater. 17 (2005) 953–961.
[19] D.R. Radu, C.Y. Lai, K. Jeftinija, E.W. Rowe, S. Jeftinija, V.S.Y. Lin, J. Am. Chem. Soc. 126 (2004) 13216–13217.
[20] T.H. Chung, S.H. Wu, M. Yao, C.W. Lu, Y.S. Lin, Y. Hung, C.Y. Mou, Y.C. Chen, D.M. Huang, Biomaterials 28 (2007) 2959–2966.
[21] I.I. Slowing, B.G. Trewyn, V.S.Y. Lin, J. Am. Chem. Soc. 128 (2006) 14792–14793.
[22] J. Lu, M. Liong, J.I. Zink, F. Tamanoi, Small 3 (2007) 1341–1346.
[23] F. Lu, S.H. Wu, Y. Hung, C.Y. Mou, Small 5 (2009) 1408–1413.
[24] J. Zhu, J.W. Tang, L.Z. Zhao, X.F. Zhou, Y.H. Wang, C.Z. Yu, Small 6 (2010) 276–282.
[25] L.M. Pan, Q.J. He, J.N. Liu, Y. Chen, M. Ma, L.L. Zhang, J.L. Shi, J. Am. Chem. Soc. 134 (2012) 5722–5725.
[26] Z.A. Qiao, L. Zhang, M. Guo, Y. Liu, Q.S. Huo, Chem. Mater. 21 (2009) 3823–3829.

[27] J. Zhu, H.X. Wang, L. Liao, L.Z. Zhao, L. Zhou, M.H. Yu, Y.H. Wang, B.H. Liu, C.Z. Yu, Chem. Asian J. 6 (2011) 2332–2338.
[28] M. Marsh, H.T. McMahon, Science 285 (1999) 215–220.
[29] S.C. Silverstein, R.M. Steinman, Z.A. Cohn, Annu. Rev. Biochem. 46 (1977) 669–722.
[30] S.L. Schmid, L.L. Carter, J. Cell Biol. 111 (1990) 2307–2318.
[31] J.L. Vivero-Escoto, I.I. Slowing, B.G. Trewyn, V.S.Y. Lin, Small 6 (2010) 1952–1967.
[32] M.A. Dobrovolskaia, S.E. McNeil, Nat. Nanotechnol. 2 (2007) 469–478.
[33] I.H. Madshus, K. Sandvig, S. Olsnes, B. Vandeurs, J. Cell Physiol. 131 (1987) 14–22.
[34] J.E. Heuser, R.G.W. Anderson, J. Cell Biol. 108 (1989) 389–400.
[35] J.M. Larkin, M.S. Brown, J.L. Goldstein, R.G.W. Anderson, Cell 33 (1983) 273–285.
[36] K. Simons, E. Ikonen, Nature 387 (1997) 569–572.
[37] H. Meng, S. Yang, Z.X. Li, T. Xia, J. Chen, Z.X. Ji, A.E. Nel, ACS Nano 5 (2011) 4434–4447.
[38] P. Thomsen, K. Roepstorff, M. Stahlhut, B. van Deurs, Mol. Biol. Cell 13 (2002) 238–250.
[39] M.L. Torgersen, G. Skretting, B. van Deurs, K. Sandvig, J. Cell Sci. 114 (2001) 3737–3747.
[40] B. Kang, S.Q. Chang, Y.D. Dai, D.C. Yu, D. Chen, Small 6 (2010) 2362–2366.